NUMERICAL SIMULATION OF IMPACT ON CERAMIC ARMOUR SYSTEM

The work reports on numerical simulation of impact problems on ceramic/aramid armour systems backed with Kevlar 29. Tests were performed with STANAG 2920 fragments and NATO 5.56 bullets driven at velocities up to 1100m/s. In order to obtain the best ballistic efficiency of the composite armour system three configurations of the armour system was taken into account in numerical simulations, varying the thickness of ceramic front plate. The thickness of backed plate was maintained constant at 2 mm. The configurations are contemplated in the table 1.

Table 1

Configuration	Ceramic/Kevlar thickness ratio (h_1/h_2)
C1	5
C2	7.5
C3	9.5

The ballistic performance of the lightweight armour systems was examined to obtain an estimate for the global damage of the composite plates.

Material models

The Mohr-Coulomb (MC) strength model and linear equation of state (EOS) are used to model the ceramic layer. The micro mechanical failure of ceramic is modelled using a cumulative damage model. Since experiments indicate that ceramics show a marked increase in compressive strength as the hydrostatic pressure is increased, it is most likely that this model will be used in conjunction with the Mohr-Coulomb model which uses a yield strength that is a function of the local hydrostatic pressure.

An advanced orthotropic model [1] implemented in Autodyn hydrocode, which use non-linear equation of state in conjunction with an orthotropic stiffness matrix is used to model the Kevlar 29/Epoxy layer.

The 4340 steel used for STANAG fragments was represented using the Johnson Cook strength model, which include strain and strain rate hardening and thermal softening effects.

A model of the NATO 5.56 bullet was developed using material data available from existing Autodyn model libraries and parameters modified based upon the measured hardness of the bullet´s individual components. The bullet is of three-part construction with a hard steel tip a relatively soft lead core and a cooper-alloy gilding jacket. There is a small gap between the front of the steel tip and the gilding jacket. The nominal mass of the bullet is 4.0 g and it has an average velocity of 1100 m/s when fired from a standard proof mount and with a standard cartridge case.

A shock equation of state and Johnson-Cook constitutive model was used to simulate the material response to dynamic loading of bullet´s tip with yield stress YS=1539MPa. The copper gilding metal was modelled using simple linear equation of state and Johnson-Cook constitutive model, the tield stress YS=330.75 MPa. The lead core was modelled using a simple linear equation of state and a Steinberg-Guinan constitutive model, the yield stress was set at YS=20MPa. The failure of jacket was simulated using a principle strain failure model set at 90%.

The material models and data are summed up in the following table.

Table 2 Material data

Ceramic-Gceramic (Autodyn material libraries)	
Equation of states : Linear	Strength Model:Mohr-Coulomb
Reference density (g/cm^3) ***3.43***	Pressure #1(kPa) **–5.00E5**
Bulk modulus (kPa) **1.54E8**	Pressure #2(kPa) **0.00**
Strength : *Mohr-Coulomb*	Pressure #3(kPa) **1.01E20**
Shear modulus (kPa) **8.30E7**	Pressure #4(kPa) **1.01E20**
Failure : *Cumulative Damage*	Yield Stress #1 (kPa) **0.00**
Reference Temperature (K) **300**	Yield Stress #2 (kPa) **3.80E6**
	Yield Stress #3 (kPa) **3.80E6**
	Yield Stress #4 (kPa) **3.80E6**
	Failure: Cumulative Damage
	Eff. Pl. Strain at Zero Damage: **0.01**
	Eff. Pl. Strain at Max. Damage: **0.03**
	Maximum Damage: **0.7**

KEVLAR/EPOXY - EMI	
Equation of states : *Orthotropic*	Tensile failure Stress 11 (kPa) *5.00E+04*
Sub-Equation of States : *Polynomial*	Maximum Shear Stress 12 (kpa) *1.00E+05*
Reference density (g/cm^3) *1.40*	Tensile Failure Strain 11 *0.01*
Young modulus 11 (kPa) *2.392E+05*	Tensile Failure Strain 22 *0.20*
Young modulus 22 (kPa) *6.311E+06*	Tensile Failure Strain 33 *0.20*
Young modulus 33 (kPa) *6.311E+06*	Post Failure Response *Orthotropic*
Poisons ratio 12 *0.115*	Fail 11 & 11 Only
Poisons ratio 23 *0.216*	Fail 22 &22 Only
Poisons ratio 31 *3.034*	Fail 33 & 33 Only
Strength : *Elastic*	Fail 12 & 12 and 11 Only
Shear modulus (kPa) *1.54E+06*	Fail 23 & 23 and 11 Only
Failure : *Material Stress/Strain*	Fail 31 & 31 and 11 Only
	Residual shear Stiff. Frac. *0.20*

4340 Steel	
Equation of States : *Linear*	Yield Stress (kPa) *7.92E+05*
Reference density (g/cm^3) *7.83*	Hardening constant (kPa) *5.10E+05*
Bulk modulus (kPa) *1.59E+07*	Hardening exponent *0.34*
Reference temperature (K) *300*	Strain rate constant *0.014*
Specific heat capacity (J/kgK) *477*	Thermal sofetning exponent *1.03*
Strength :*Johnson-Cook*	Melting temperature (K) *1793*
Shear modulus (kPa) *8.18E+07*	

Numerical models

As the high velocity impact phenomenon is of localised nature, the boundary conditions do not influence the results and therefore only a square region of 100 x 100 mm was modelled. Both the target and the projectiles were modelled using TrueGrid [] taking into account the symmetry of the problems. The analysis starts with the impactor and plate in contact. The modelled geometry and the initial grid are illustrated in Figure 1.

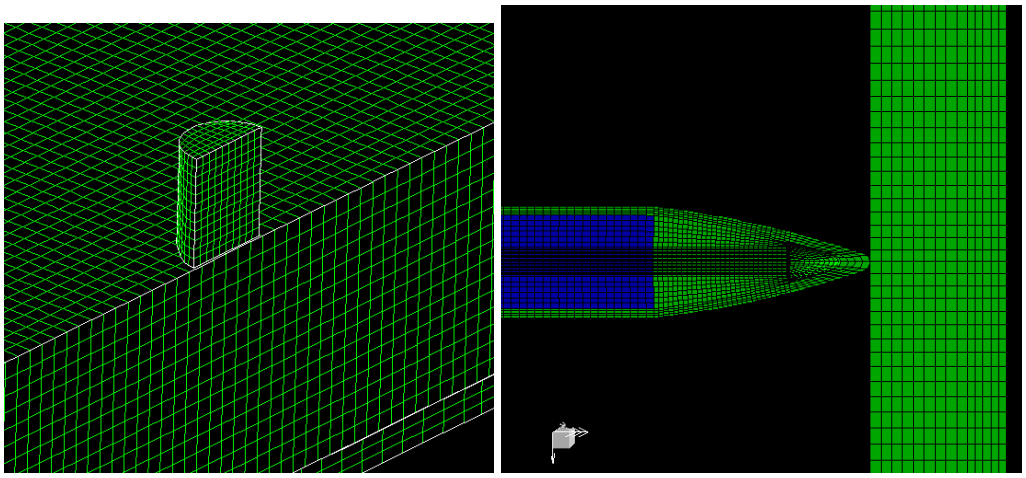

Figure 1. Numerical models for STANAG and NATO 5.56

The Lagrange processor was used to represent both projectile and composite target. This processor attaches the mesh to the material and they deforms together.
Because was used the Lagrangian scheme in numerical simulation it requires an artificial technique to treat large deformation called erosion technique. The erosion is a numerical procedure, which allows automatic removal of elements when they become heavily distorted. Degenerate cells were *eroded* at an instantaneous geometric strain equal to 1.0 for ceramic and Kevlar layers and 2 for projectiles components.

In order to capture the main events in failure processes an numerical model that use SPH meshless particle in conjunction with Lagrange hexahedral elements was also developed. Since SPH does not require a numerical grid, there is no grid-tangling problem for large deformation problems, consequently no need for erosion to obtain efficient solutions. But because under certain conditions the SPH algorithms can become unstable [ ] (numerical fracture), we failed in our tentative to model the NATO 5.56 impact problem using SPH particle to model the ceramic tail.

Numerical results

1. **Ballistic impact of STANAG fragments on Ceramic/Aramid armour systems**

	C1-10 mm	C2-15mm	C3-19 mm
Ceramic damage	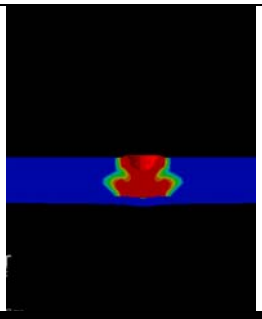	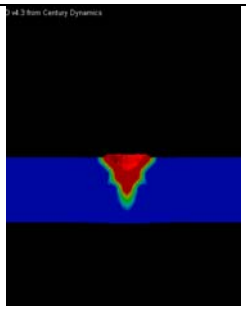	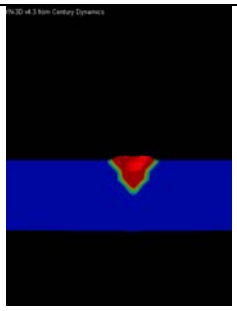
Material status	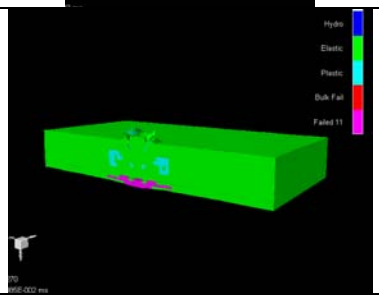	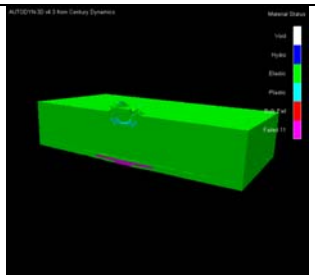	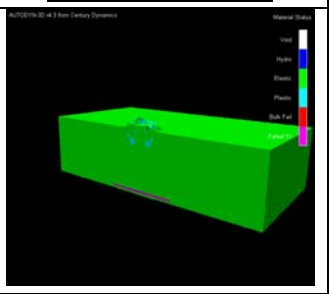

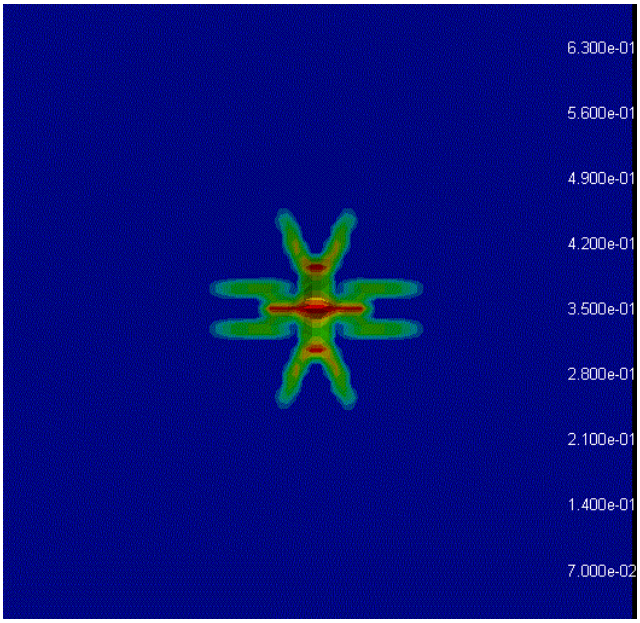

Back view of ceramic tile. Configuration C1 (10 mm ceramic tile).
Cracks development.

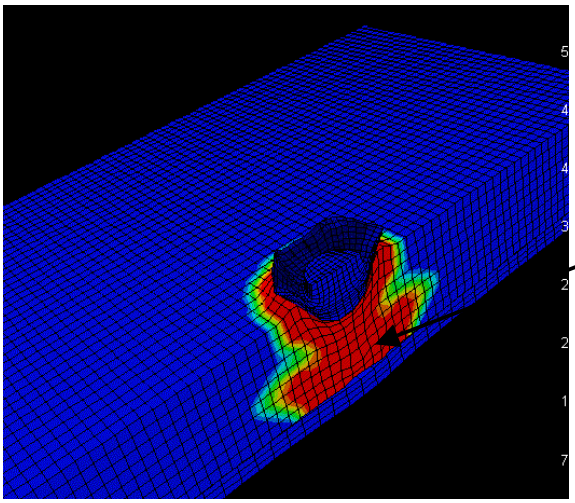

(a) Full Lagrange

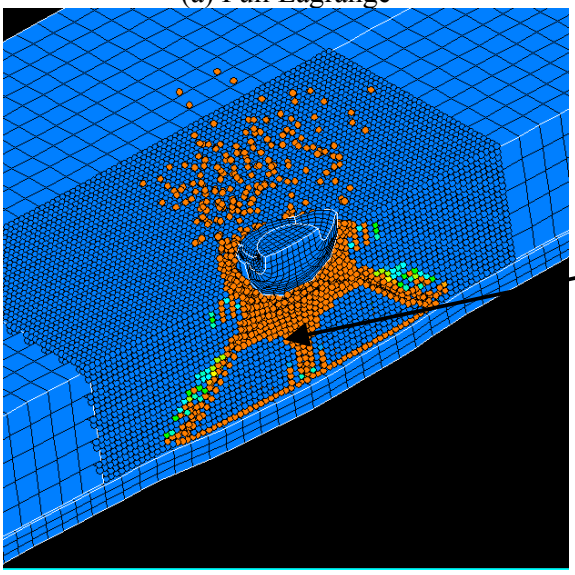

(b) SPH mesless with Lagrange elements

Comparisons of SPH (b) vs. full Lagrange (a) numerical models

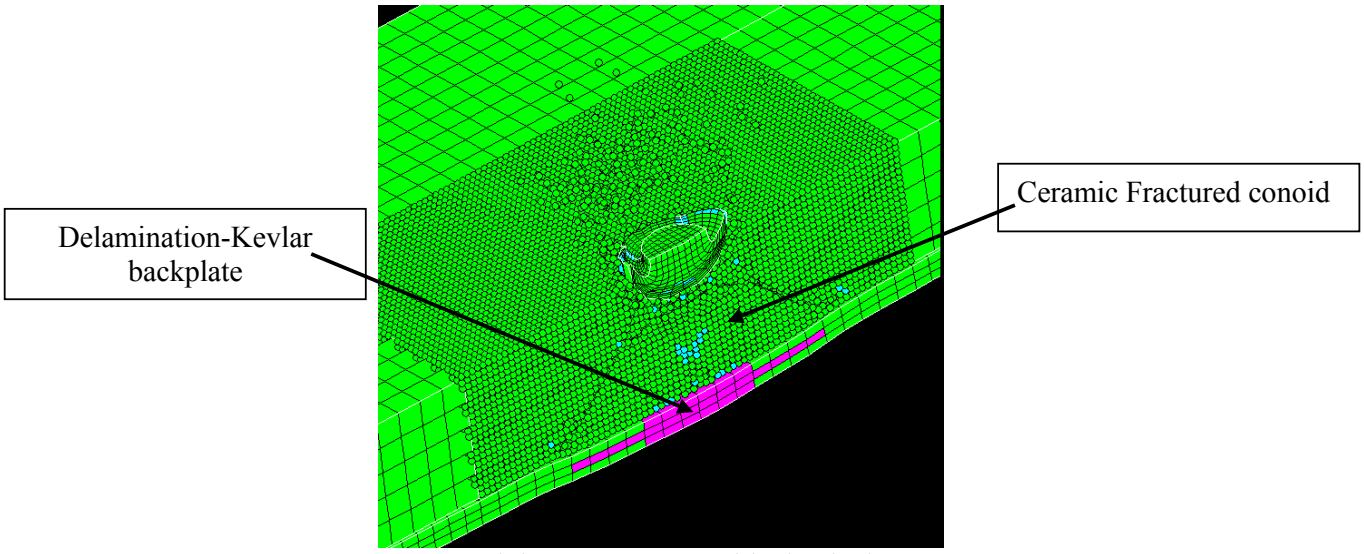

Material status at zero residual velocity

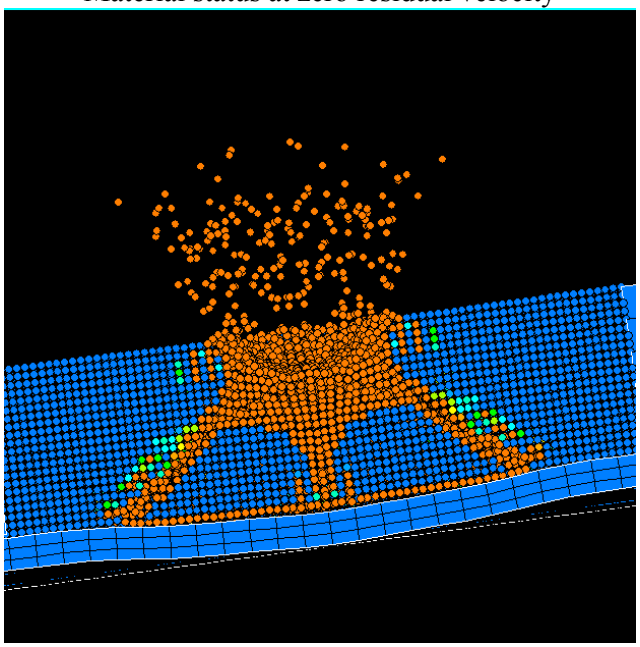

Final damage in ceramic tile (C1 configuration)

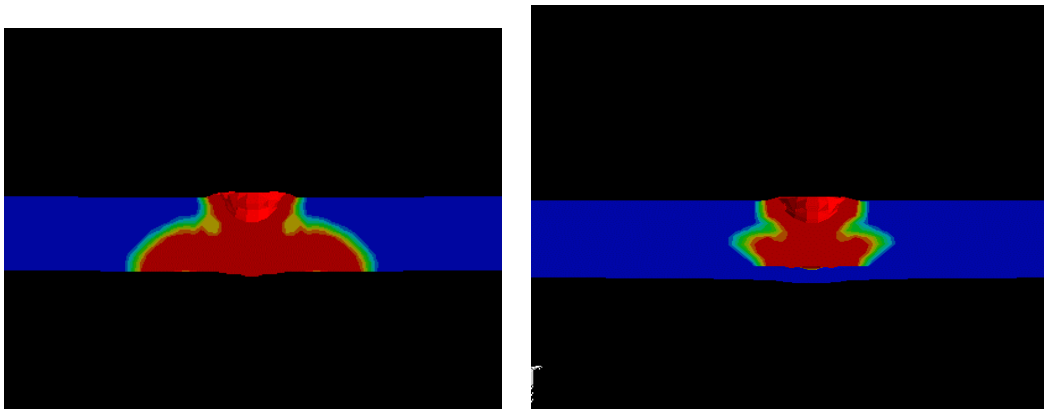

(a) (b)

Final damage in ceramic tile. (a) Without backplate (b) with Kevlar backplate

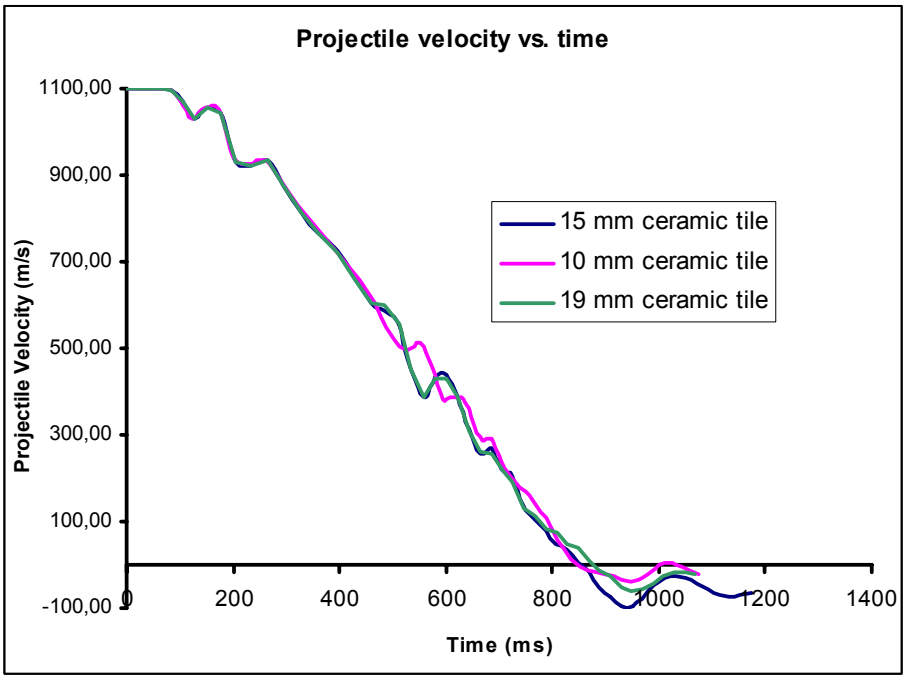

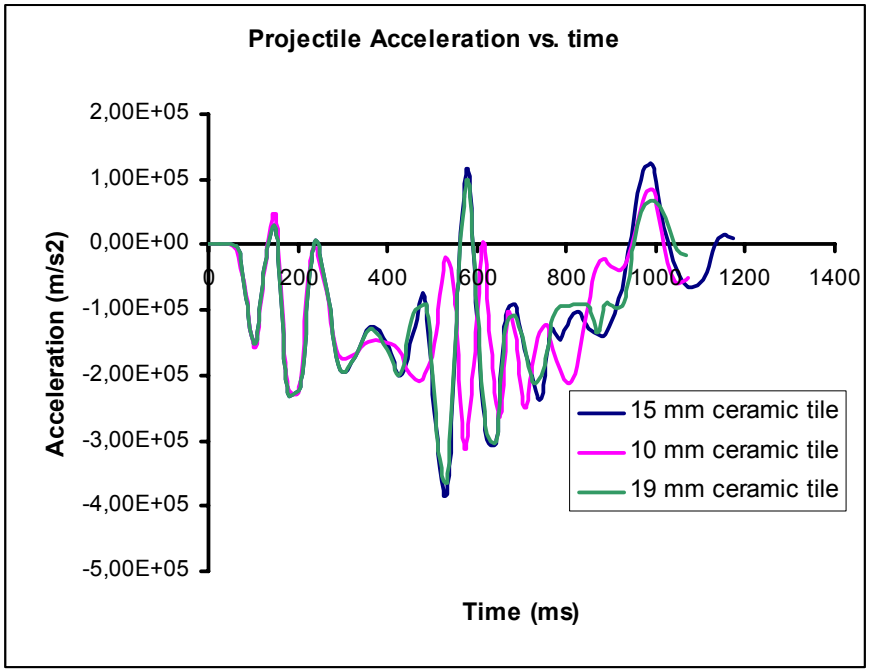
Projectile Acceleration vs. time
2,00E+05
1,00E+05
0,00E+00
-1,00E+05
-2,00E+05
-3,00E+05
-4,00E+05
-5,00E+05
Acceleration (m/s2)
0
200
400
600
800
1000
1200
1400
Time (ms)
15 mm ceramic tile
10 mm ceramic tile
19 mm ceramic tile

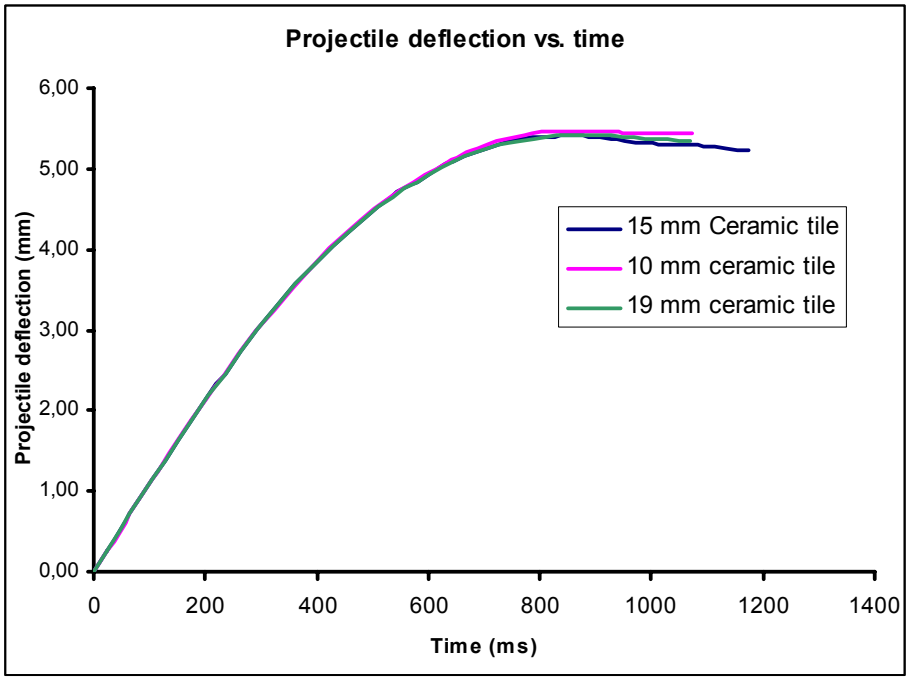
Projectile deflection vs. time
6,00
5,00
4,00
3,00
2,00
1,00
0,00
Projectile deflection (mm)
0
200
400
600
800
1000
1200
1400
Time (ms)
15 mm Ceramic tile
10 mm ceramic tile
19 mm ceramic tile

2. Ballistic impact of NATO 5.56 bullets on Ceramic/Aramid armour systems

	Configuration C1 (10 mm)	Configuration C2 (15 mm)	Configuration C3 (19mm)
Damage in ceramic	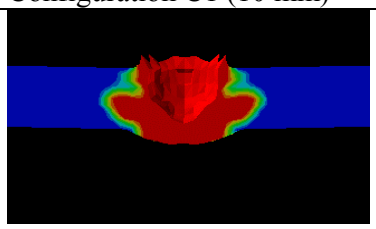	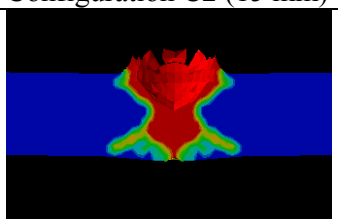	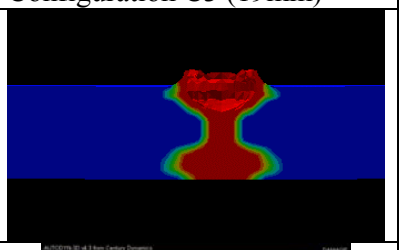
Cracks development in ceramic on back face	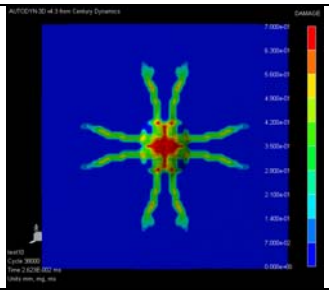	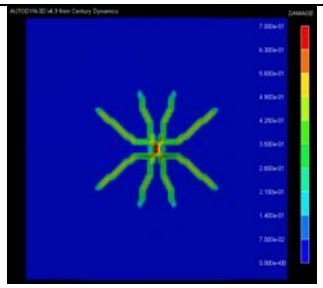	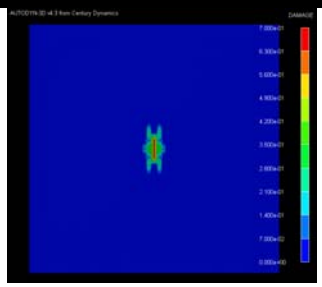

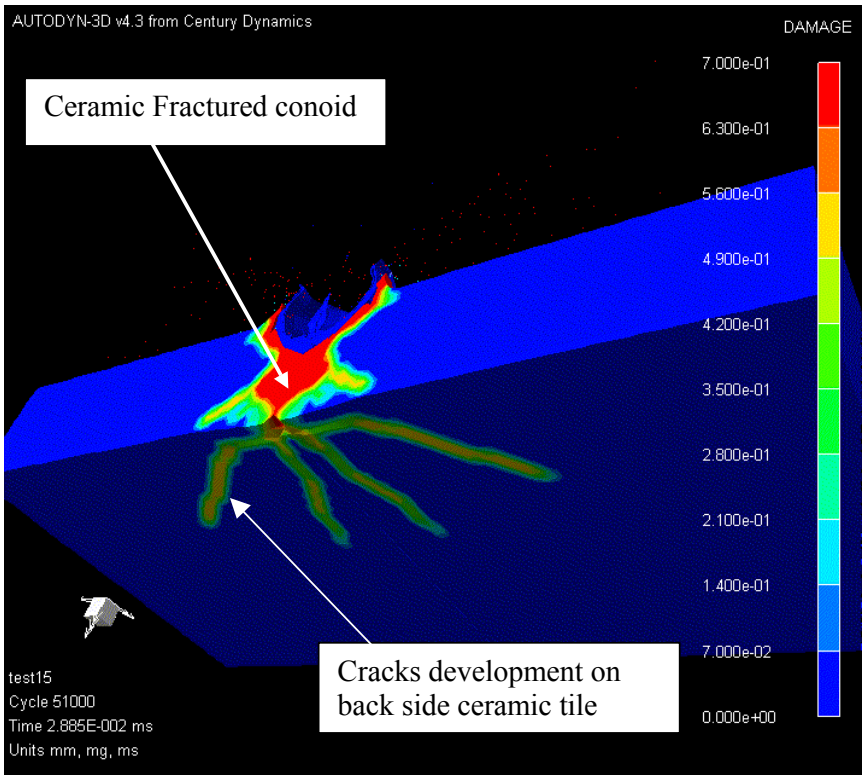

Final status of damage in ceramic tile at zero residual velocity (configuration C2)

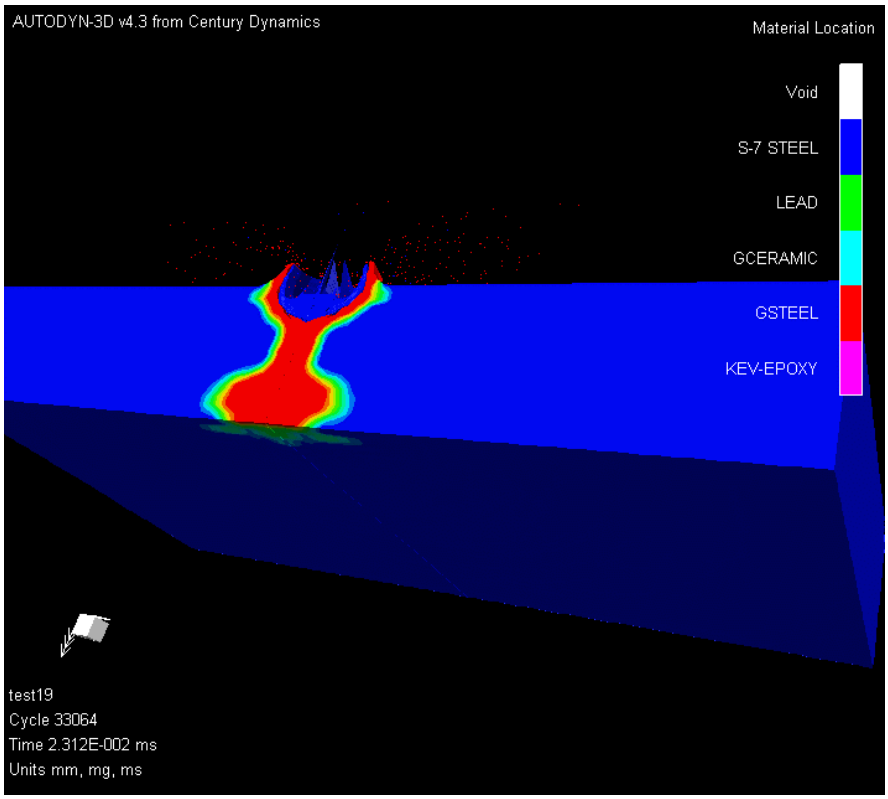

Final status of damage in ceramic tile at zero residual velocity (configuration C3)

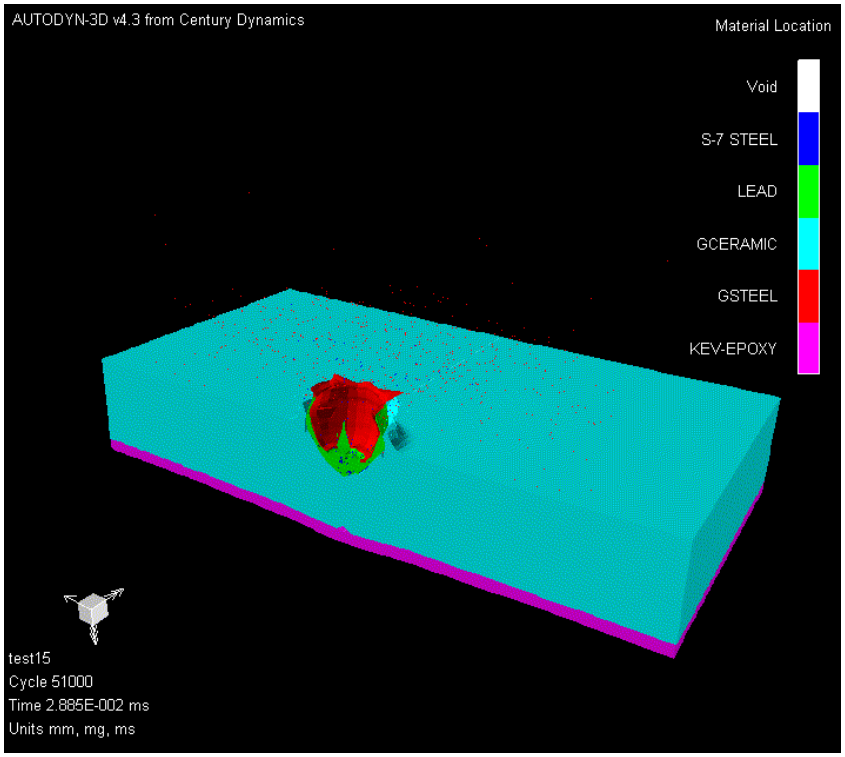

Configuration C2-Material location at zero residual velocity

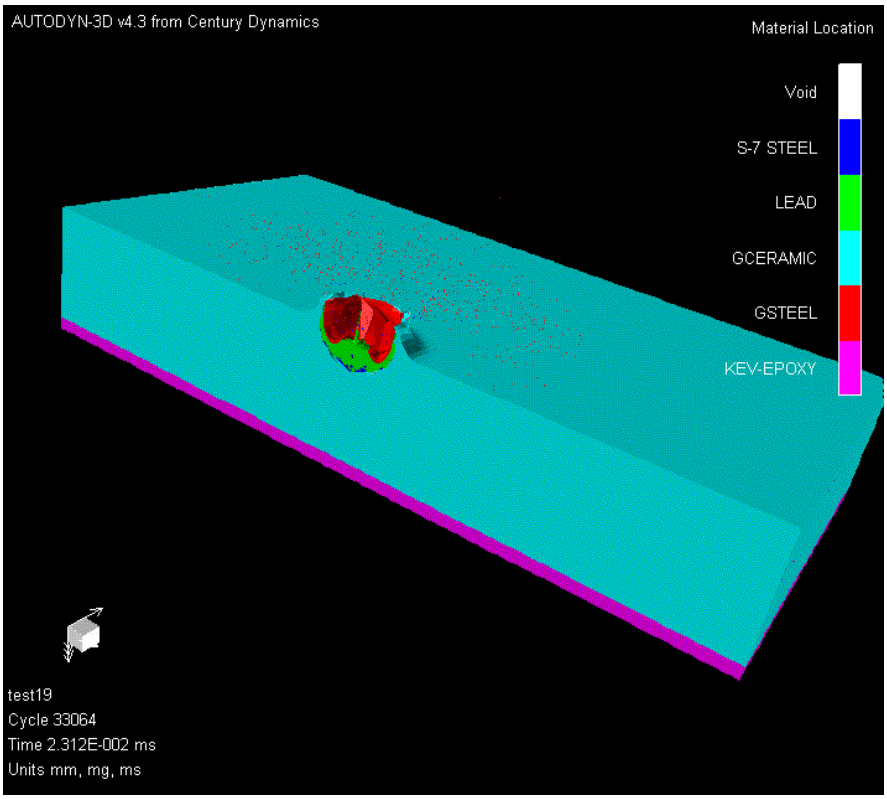

Configuration C3-Material location at zero residual velocity